BIOCHEMICAL PHARMACOLOGY 73 (2007) 1635–1645

available at www.sciencedirect.com

ScienceDirect

journal homepage: www.elsevier.com/locate/biochempharm

Capsaicin causes protein synthesis inhibition and microtubule disassembly through TRPV1 activities both on the plasma membrane and intracellular membranes

Ping Han *, *Heath A. McDonald, Bruce R. Bianchi, Rachid El Kouhen, Melissa H. Vos, Michael F. Jarvis, Connie R. Faltynek, Robert B. Moreland*

Neuroscience Research, Global Pharmaceutical Research and Development, Abbott Laboratories, Abbott Park, IL 60064, USA

ARTICLE INFO

Article history:
Received 11 October 2006
Accepted 22 December 2006

Keywords:
TRPV1
VR1
Calcium
Protein synthesis
Microtubule
Capsaicin

ABSTRACT

TRPV1 is a non-selective cationic channel that is activated by capsaicin, acidic pH and thermal stimuli. Sustained TRPV1 channel activation causes severe cytotoxicity that leads to cell death. In this study, we investigated the mechanisms of capsaicin-induced cytotoxicity in HEK293 cells stably expressing TRPV1 with a focus on protein synthesis regulation and cytoskeleton reorganization. Capsaicin inhibited protein synthesis in TRPV1-expressing HEK cells with an IC_{50} of 15.6 nM and depolymerized microtubules within 10 min after exposure. These effects were completely blocked by pretreatment of cells with the TRPV1 antagonist A-425619, both in the presence and absence of extracellular calcium. Protein synthesis inhibition induced by capsaicin was not a result of eIF2α hyperphosphorylation, but rather closely correlated with cytosolic calcium elevation caused by calcium flux through cell surface and intracellular TRPV1, and/or ER calcium depletion through intracellular TRPV1. Microtubule dependent cell process shrinkage may serve as a mechanism for rapid alteration of the neurotransmission network upon TRPV1 activation. Taken together, the present studies demonstrate that intracellular pool of TRPV1 plays an important role in regulating cell morphology and viability upon receptor activation.

1. Introduction

TRPV1 is a non-selective, ligand-gated, cationic channel that can be activated by capsaicin, noxious heat and protons [1]. It is expressed primarily on small diameter nociceptive neurons that integrate responses to multiple noxious stimuli [2,3]. In addition to peripheral sensory neurons, TRPV1 mRNA, protein and function are also detected in central nervous system as well as in non- neuronal cell types including epithelial cells from respiratory tissues, bladder and tongue [4–6]. TRPV1 gene knockout in mice, and TRPV1 receptor antagonism in rat both result in reduced thermal hyperalgesia in response to inflammation, suggesting that TRPV1 plays a pathological role in pain sensation [7–12]. Endogenous ligands anandamide, *N*-arachidonoyl-dopamine (NADA), *N*-oleoyldopamine (OLDA) (which are also agonists of cannabinoid receptor CB1), and 12-hydroperoxytetraenoic acid (12-HPETE) (which is the product of lipoxygenase), have also been shown to activate TRPV1

* *Corresponding author*. Tel.: +1 847 935 5339; fax: +1 847 937 9195.
E-mail address: ping.han@abbott.com (P. Han).

Abbreviations: TRPV, transient receptor potential channel type V; VR1, vanilloid receptor 1; CAP, capsaicin; DRG, dorsal root ganglion; FLIPR, Fluorometric Imaging Plate Reader; DOC, deoxycholic acid; NP-40, Nonidet P-40; ER, endoplasmic reticulum; PM, plasma membrane; $[Ca^{2+}]_i$, intracellular calcium levels; $[Ca^{2+}]_o$, extracellular calcium levels; RTX, resiniferatoxin; CPZ, capsazepine; A-425619, 1-isoquinolin-5-yl-3-(4-trifluoromethyl-benzyl)-urea; RR, ruthenium red

0006-2952/$ – see front matter
doi:10.1016/j.bcp.2006.12.035

[13–15]. Thus, TRPV1 is involved in multiple cellular processes and is regulated via complicated signal transduction pathways.

TRPV1 activation leads to neuron desensitization and even neuron damage depending on the strength of stimulation and the duration of activation [16–19]. This cytotoxic property has been clinically applied to relieve bladder over-reactivity and pain [20,21]. TRPV1 mediated cytotoxicities have been found to include DNA fragmentation, protein synthesis inhibition, cytokine production, caspase activation and lipid metabolism [22–25]. Recent studies on the mechanisms of TRPV1-mediated cytotoxicities were primarily focused on TRPV1 channels located on the plasma membrane ($TRPV1_{PM}$). However, over 90% of TRPV1 channels are localized on the intracellular membrane compartment (such as $TRPV1_{ER}$), and are also functional in response to agonist stimulation [26–28]. Upon ligand binding, intracellular TRPV1 is able to translocate calcium ions from intracellular calcium stores into cytosolic compartment [26,27]. However, the physiological consequences of intracellular TRPV1 activation remain obscure. In this study, we focused on the involvement of intracellular TRPV1 on protein synthesis and cytoskeleton integrity, two processes that are highly dependent on cellular calcium homeostasis. Our observation provides insight into the potential role of intracellular TRPV1 on cytotoxicity, revealing the cellular processes that are involved in TRPV1-mediated cell death.

2. Materials and methods

2.1. Cell line stably expressing recombinant rat TRPV1

HEK 293 cells were maintained in DMEM medium (Invitrogen, Carlsbad, CA) supplemented with 10% FBS (Hyclone, Logan, UT), 2 mM glutamine and 1× Penicillin–Streptomycin (Invitrogen, Carlsbad, CA). 24 h before transfection, cells were split into 6 cm tissue culture plates. Five micrograms of pCIneo-rTRPV1 plasmid DNA previously described [29] was transfected into the cells using Lipofectamine reagent according to manufacturer's instructions (Invitrogen, Carlsbad, CA). Forty-eight hours after transfection, cells were split 1:10 into selection medium containing 0.3 mg/ml Geneticin (Invitrogen, Carlsbad, CA). Geneticin resistant colonies were picked 10 days later. The homogeneity and purity of the cell population in each colony were further determined by immunofluorescence using anti-TRPV1 antibody. The HEK rat TRPV1/C2 cell line contained over 95% TRPV1 positive cells was amplified and used for biochemical and pharmacological characterization of rat TRPV1.

2.2. Antibodies

Two different TRPV1 antibodies were used in this study. ABRK1 antibody was raised against peptide SRTRLFGKGDSEEAC corresponding to amino acids 45–58 of human and rat TRPV1 from Anaspec (San Jose, CA) [30]. TRPV1 P-19 antibody raised against the N-terminal region of rat TRPV1 in goat was obtained from Santa Cruz Biotechnology (Santa Cruz, CA). eIF2α pan antibody (AHO0821) and S51 phosphospecific antibody (PHF0024) were obtained from Biosource (Camarillo, CA). α-Tubulin monoclonal antibody was from Sigma–Aldrich (St. Louis, MO).

2.3. FLIPR assay

Capsaicin evoked calcium flux was measured by Fluorometric Imaging Plate Reader (FLIPR; Molecular Devices, Sunnyvale, CA) as described previously [29]. Briefly, cells were plated into 96 well black wall Bio-coat tissue culture plates at the density of 50,000 cells/well 24 h before assay. After the cells were preloaded with 1.14 μM fluo-4 AM (Invitrogen, Carlsbad, CA) for 2 h, cells were washed with DPBS (2× 0.25 ml) to remove extracellular fluo-4 AM. Fluorescent readings were made over a 4 min period at 1–5 s intervals following addition of agonist to the cells. Antagonist was added 3 min before addition of agonist. Capsaicin (Sigma–Aldrich, St. Louis, MO) and Resiniferatoxin (LKT Laboratories, St. Paul, MN) were used as TRPV1 agonists. TRPV1 antagonist capsazepine was from Sigma–Aldrich (St. Louis, MO) and A-425619 was synthesized in Abbott Laboratories (Abbott Park, IL). The peak increase in relative fluorescent units over the baseline fluorescence was calculated for each well, and expressed as a percentage of the maximum response to TRPV1 agonist. Concentration–response data were analyzed using a four-parameter logistic Hill equation in GraphPad Prism (San Diego, CA).

2.4. Immunoprecipitation and Western blot analysis

HEK rat TRPV1/C2 cells were harvested and lysed in PBS buffer containing 0.5% DOC and 0.5% NP-40 on ice for 10 min to extract both cytosolic and membrane bound proteins. Two hundred micrograms of cell lysate was diluted to 1 ml with PBS for each immunoprecipitation assay. Four microliters of ABRK1 antibody was added to the diluted cell lysate followed by continuous rotation for more than 3 h at 4 °C. Thirty microliters of protein A agarose beads (Invitrogen, Carlsbad, CA) were subsequently added to capture the immune complex. Following centrifugation, the beads were washed with buffer containing 37.5 mM NaCl, 2.5 mM Tris 8.3, 1.25 mM EDTA, 0.025% Triton X-100 and 1× complete protease inhibitors cocktail (Roche, Indianapolis, IN) for 4× 10 min at 4 °C. Protein was eluted from protein A agarose beads by adding SDS sample buffer and heating at 100 °C for 3 min. Immunoprecipitated TRPV1 protein was fractionated on 4–12% Bis–Tris SDS-PAGE (Invitrogen, Carlsbad, CA) and transferred onto PVDF membrane (Invitrogen, Carlsbad, CA) for Western blot analysis. Goat anti-TRPV1 N-terminal P-19 antibody diluted 1:300 was used to detect TRPV1 protein. The immune reactive signals were detected by HRP conjugated secondary antibody and ECL-plus (Amersham Bioscience, Buckinghamshire, UK).

2.5. Protein synthesis assay

HEK 293 or HEK rat TRPV1/C2 cells were plated onto 24 well plates 48 h before protein synthesis assay. Prior to the assay, cells were rinsed and incubated in starvation medium (methionine- and cystine-free DMEM medium supplemented with 2 mM L-glutamine, obtained from Invitrogen Carlsbad, CA) for 15 min to deplete the methionine and cystine. Then, 200 μl of EasyTag EXPRESS [^{35}S] Protein Labeling Mix (Perkin-Elmer, Boston, MA) prepared in starvation medium at the concentration of 10 μCi/ml together with TRPV1 agonist, antagonists and/or calcium chelator EGTA were added to

each well to metabolic label newly synthesized protein. EGTA and non-selective channel blocker ruthenium red (RR) were from Sigma–Aldrich (St. Louis, MO). After 1-h incubation at 37 °C, the medium was removed and the cells were washed and harvested into clean tubes. Following centrifugation at 1000 × *g* for 3 min at 4 °C, the cell pellets were resuspended in protein extraction buffer containing 150 mM NaCl, 50 mM Tris 8.8, 6 mM EDTA, 2.5% Triton X-100, 5 mM methionine, 5 mM cysteine and 1 mg/ml BSA to extract the total cellular proteins. After centrifugation at 10,000 × *g* for 10 min at 4 °C, the soluble cell extracts were transferred to a clean tube and were precipitated with acetone at final concentration of 80% for 10 min at room temperature. Precipitates protein were centrifuged at 10,000 × *g* for 5 min and were washed once with 80% acetone to remove unincorporated radioactivities. Protein pellets were resolubilized in 50 μl of PBS buffer containing 2% SDS. Ten microliters of the protein solution was mixed with 1 ml EcoLume scintillation fluid (ICN, Costa Mesa, CA) and counted in LS 6500 Multi-purposes scintillation counter (Beckman Coulter, Fullerton, CA) for 1 min.

2.6. Microtubule structure

HEK rat TRPV1/C2 cells were cultured in chamber #1.5 coverglasses (Nalge Nunc International Corp., Naperville, IL) for 2 days in 37 °C/5% CO_2 tissue culture incubator and were rinsed with HBSS buffer (Invitrogen, Carlsbad, CA) right before staining. After treating cells with 200 nM capsaicin for 10 min, or 10 μM A-425619 5 min before capsaicin treatment, TubulinTracker (Oregon Green 488 Taxol), the fluorescent live cell microtubule-binding reagent (Invitrogen, Carlsbad, CA) was mixed with 20% Pluronic F-127 (Invitrogen, Carlsbad, CA) and applied to the cells at the final concentration of 250 nM. Cells were incubated with TubulinTracker at 37 °C for 30 min and were then rinsed with pre-warmed HBSS buffer. Microtubule structure was immediately observed under the confocal microscope.

2.7. Confocal microscopy

Microtubules stained with TubulinTracker were observed with Zeiss LSM5 PASCAL inverted confocal microscope (Carl Zeiss

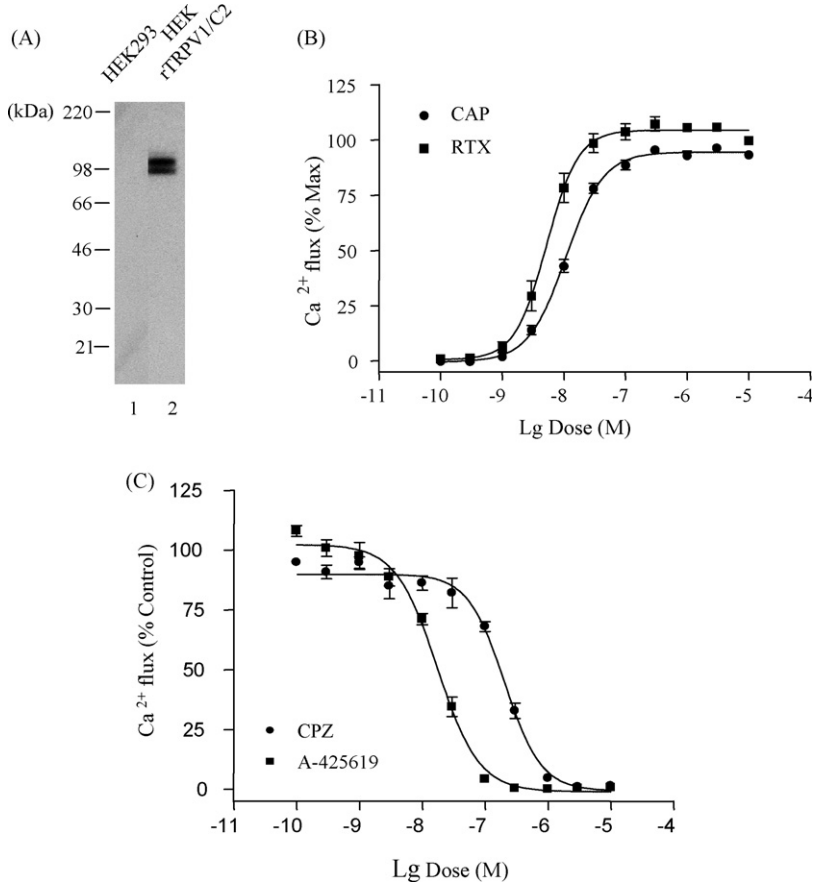

Fig. 1 – Characterization of HEK rTRPV1/C2 stable cell line. (A) Determination of rat TRPV1 protein expression by Western blot analysis. TRPV1 protein was immunoprecipitated from 200 μg of total protein lysate prepared from untransfected HEK 293 cells or HEK rTRPV1/C2 cells using ABRK1 antibody. The immunoprecipitates were fractionated on 4–12% Bis–Tris Nupage gel and blotted with TRPV1 P-19 antibody. (B) Dose–response curves of capsaicin and Resiniferatoxin (RTX) induced calcium flux measured by FLIPR assay in HEK rTRPV1/C2 cell line. EC_{50} for capsaicin and Resiniferatoxin are calculated to be 11.3 ± 0.9 and 5.71 ± 1.01 nM, respectively. (C) Dose–response curves of TRPV1 inhibitors capsazepine and A-425619 to attenuate 20 nM capsaicin induced calcium influx in FLIPR assay in HEK rTRPV1/C2 cell line. K_i values for capsazepine and A-425619 are calculated to be 74.73 ± 6.86 and 6.32 ± 0.54 nM, respectively. Data represented mean ± standard deviation (*n* = 6–10).

MicroImaging, Inc., Thornwood, NY). Images were captured with αPlan-Fluar 100× oil lenses (numerical aperture, 1.45). Live cell calcium imaging studies of HEK rat TRPV1/C2 cells were recorded using Time Series Macro with 3 s (Fig. 5A) and 6 s intervals (Fig. 5B), respectively. Images were captured with LD Plan-Neofluar 40× air lenses (numerical aperture, 0.6). Fluorescent intensities were measured at 12-bit depth by confocal microscope on selected regions of interest (ROIs). The whole recording lasted for 1800 s and the fluorescence changes of the first 600 and 800 s are plotted in Fig. 5A and B, respectively.

3. Results

3.1. Characterization of HEK rat TRPV1/C2 stable cell line

HEK293 cells stably expressing rat TRPV1 (HEK rTRPV1/C2) were established to study the cellular events involved in TRPV1 activation. Full-length rat TRPV1 protein was expressed in HEK rTRPV1/C2 cell line but not in untransfected HEK293 cells. This was determined by immunoprecipitation with TRPV1 N-terminal antibody ABRK-1 followed by Western blot analysis using TRPV1 P-19 antibody (Fig. 1A). Application of capsaicin to HEK rTRPV1/C2 cells initiated a marked elevation of $[Ca^{2+}]_i$ (Fig. 1B), while no response was detected in untransfected HEK293 cells (data not shown). Dose–response curves using capsaicin and Resiniferatoxin showed that these agonists stimulated calcium influx in HEK rTRPV1/C2 stable cells with EC_{50} values of 11.3 ± 0.9 nM (n = 10) and 5.71 ± 1.01 nM ($n = 6$), respectively (Fig. 1B). Capsaicin (20 nM) evoked calcium flux was inhibited by pre-treating cells with the TRPV1 antagonist capsazepine ($K_i = 74.73 \pm 6.86$ nM, $n = 6$) or A-425619 ($K_i = 6.32 \pm 0.54$ nM, $n = 6$) (Fig. 1C).

3.2. Capsaicin treatment inhibits total cellular protein synthesis

Elevation of intracellular calcium concentration usually correlates with protein synthesis inhibition [31]. To study whether capsaicin evoked $[Ca]_i$ elevation through TRPV1 activation inhibits protein synthesis, and whether this contributes to capsaicin cytotoxicity, total protein synthesis was measured in the HEK rTRPV1/C2 cell line. Protein synthesis was determined by incorporation of $[^{35}S]$-methionine in metabolic labeling experiments. In the absence of capsaicin, newly synthesized protein increased linearly with time, with 72.7 ± 5.4 fmoles ($n = 2$) of $[^{35}S]$-methionine incorporated per 10^6 cells in 60 min. Treatment with 200 nM capsaicin reduced $[^{35}S]$-methionine incorporation to 14.7 ± 0.4 fmoles ($n = 2$) per 10^6 cells in the same time period (Fig. 2A). Plot of $[^{35}S]$-methionine incorporation versus capsaicin showed that capsaicin inhibited total protein synthesis in HEK rat TRPV1/C2 cells in a concentration dependent manner with an IC_{50} value of 15.6 ± 1.9 nM ($n = 3$); but had no effect on untransfected HEK 293 cells (Fig. 2B).

3.3. Capsaicin inhibits protein synthesis both in the presence and absence of extracellular calcium

To investigate the role of TRPV1 plays in capsaicin-induced protein synthesis inhibition, total protein synthesis was studied in the presence of TRPV1 agonist capsaicin and/or antagonist A-425619 [32]. Treatment with 200 nM capsaicin reduced protein synthesis to 13.6 ± 2.5% ($n = 13$) in HEK rTRPV1/C2 cells compared to a no capsaicin treatment (Fig. 3A). Pre-incubation of cells with either 1 or 10 μM of the TRPV1 specific antagonist A-425619 for 5 min prior to capsaicin treatment reversed the inhibition of protein synthesis to 112 ± 15.18% ($n = 3$) and 109.5 ± 22.2% ($n = 3$) of control, respectively. A-425619 at 10 μM showed no effect on its own (120.5% ± 8.6%, $n = 3$ of control remained) (Fig. 3A). This result is consistent with capsaicin inhibiting protein synthesis through TRPV1 activation.

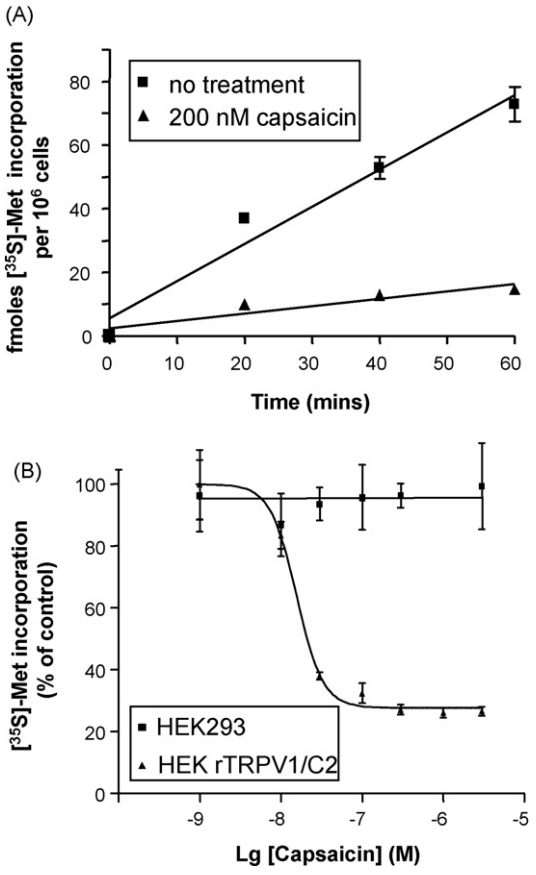

Fig. 2 – Capsaicin inhibits protein synthesis in TRPV1 expressing cells. (A) Capsaicin inhibited total protein synthesis in HEK rTRPV1/C2 cells. Total protein synthesis was measured with $[^{35}S]$-methionine metabolic labeling in HEK rTRPV1/C2 cells in the absence or presence of 200 nM capsaicin for 20, 40 and 60 min. Femto moles of $[^{35}S]$-methionine incorporation per 10^6 cells were plotted against the function of time. Data represented mean ± S.E.M. from two independent experiments. (B) Capsaicin inhibits protein synthesis via TRPV1 receptor. Dose–response effects of capsaicin on protein synthesis were studied in untransfected HEK 293 and HEK rTRPV1/C2 cells. Newly synthesized protein was measured by $[^{35}S]$-methionine incorporation over a period of 60 min. Data represented mean ± S.E.M. from three independent experiments.

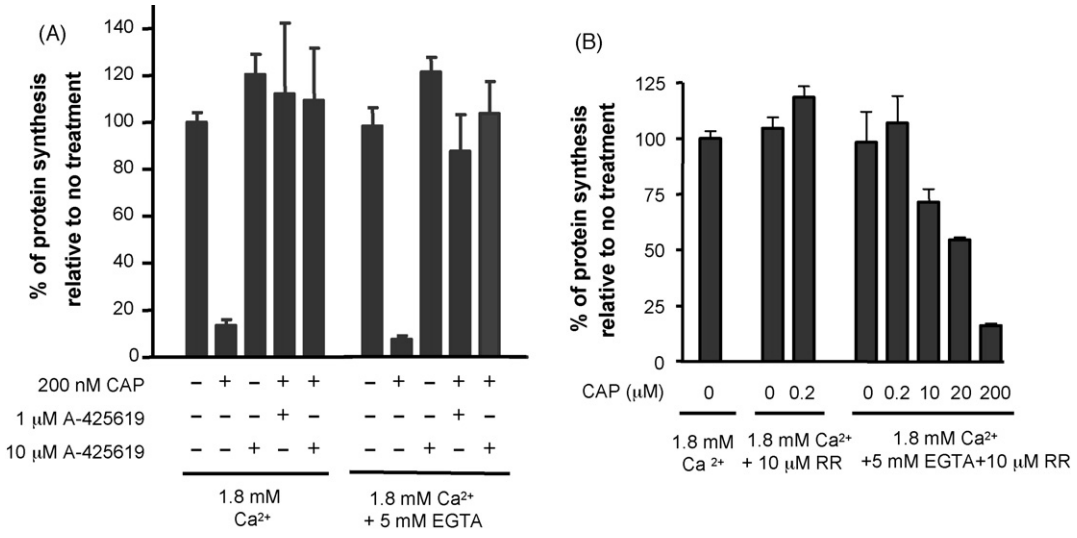

Fig. 3 – Determination of protein synthesis rates under different cellular calcium levels. (A) Protein synthesis levels of HEK rTRPV1/C2 cells in the presence of 200 nM capsaicin, 5 mM EGTA, 1 or 10 μM of A-425619 either alone or in different combinations were measured by [^{35}S]-methionine incorporation. (B) Protein synthesis levels of HEK rTRPV1/C2 cells in response to capsaicin and 10 μM of ruthenium red (RR) either in the absence or presence of 5 mM EGTA were measured by [^{35}S]-methionine incorporation. The percentages of newly synthesized protein relative to untreated cells were plotted. Data represented mean ± S.E.M. (n = 3–13).

To determine how $TRPV1_{PM}$ versus $TRPV1_{ER}$ are involved in protein synthesis inhibition, 5 mM EGTA was included in the metabolic labeling medium to chelate the extracellular calcium. The presence of 5 mM EGTA reduced extracellular free calcium from 1.8 mM to 0.0224 μM (calculated using EGTA calculator [33]), which is about 5-fold lower than cellular calcium concentrations under steady state (10^{-7} M) and is considered as zero $[Ca^{2+}]_o$. Under these conditions, 98.4 ± 7.9% (n = 13) of protein synthesis remained during 60 min of metabolic labeling. However, treating cells with 200 nM capsaicin and 5 mM EGTA together reduced protein synthesis to 7.6 ± 1.58% (n = 13) of control (Fig. 3A). Pretreatments with 1 or 10 μM A-425619 was able to reverse protein synthesis inhibition to 87.7 ± 15.6% (n = 3) and 103.8 ± 13.65% (n = 3) of control, respectively (Fig. 3A). These results suggested that capsaicin induced protein synthesis may not be solely mediated by cytosolic calcium increment, depletion of intracellular calcium store, such as ER, through $TRPV1_{ER}$ might also play a role.

To further evaluate the contribution of $TRPV1_{ER}$ to capsaicin induced protein synthesis inhibition, 10 μM ruthenium red was used together with 5 mM EGTA to ensure no calcium influx from extracellular source [27]. Unlike A-425619 that is permeable through cell and inhibits TRPV1 both on the plasma membrane and on the intracellular membrane compartment, ruthenium red has limited membrane permeability. Ruthenium red preferentially inhibits cell surface channels but has reduced efficacy on intracellular channels. It has been reported that, 0.1 μM ruthenium red completely blocked 10 μM capsaicin induced calcium influx through cell surface $TRPV1_{PM}$. However, 10 μM of ruthenium red was only sufficient to block $TRPV1_{ER}$ induced by low concentration of capsaicin (<1 μM), but not high concentration of capsaicin (>20 μM) under zero $[Ca^{2+}]_o$ condition [27]. When we included the 10 μM of ruthenium red in the metabolic labeling medium, it has no effect toward total protein synthesis alone, regardless of extracellular calcium. 104.6 ± 4.9% (n = 3) and 98.3 ± 13.8% (n = 3) of protein synthesis relative to control remained in the absence and presence of 5 mM ETGA, respectively (Fig. 3B). Ten micromolar of ruthenium red also reversed 200 nM capsaicin induced protein synthesis inhibition both in the absence and presence of 5 mM EGTA, 118.6 ± 4.8% (n = 3) and 107.1 ± 12.0% (n = 3) of protein synthesis relative to control remained, respectively (Fig. 3B). When capsaicin concentration was elevated to 10, 20 and 200 μM, the concentrations known to cause calcium efflux out of ER in the presence of ruthenium red [27], total protein synthesis was reduced to 71.5 ± 5.7, 54.6 ± 1.0 and 16.3 ± 0.9% (n = 3), respectively (Fig. 3B). Taken together, based on the results of both A-425619 and ruthenium red, we concluded that, capsaicin induced protein synthesis inhibition was primarily due to calcium efflux out of the ER compartment through $TRPV1_{ER}$ under zero $[Ca^{2+}]_o$ condition.

3.4. *Capsaicin treatment causes microtubules depolymerization*

The microtubule structure in TRPV1-expressing cells upon capsaicin treatment was studied using TubulinTracker that binds the polymerized microtubules [34]. After treating cells with 200 nM capsaicin for 10 min in DPBS buffer containing 0.9 mM $CaCl_2$, microtubules were severely depolymerized. The long fiber like structures of microtubules shrank into short spikes and small dots (Fig. 4A and B). If cells were treated with TubulinTracker before capsaicin exposure, the Taxol–microtubule complexes were resistant to capsaicin and remained polymerized (data not shown). Pretreatment of cells with 10 μM A-425619 was able to block capsaicin induced microtubule

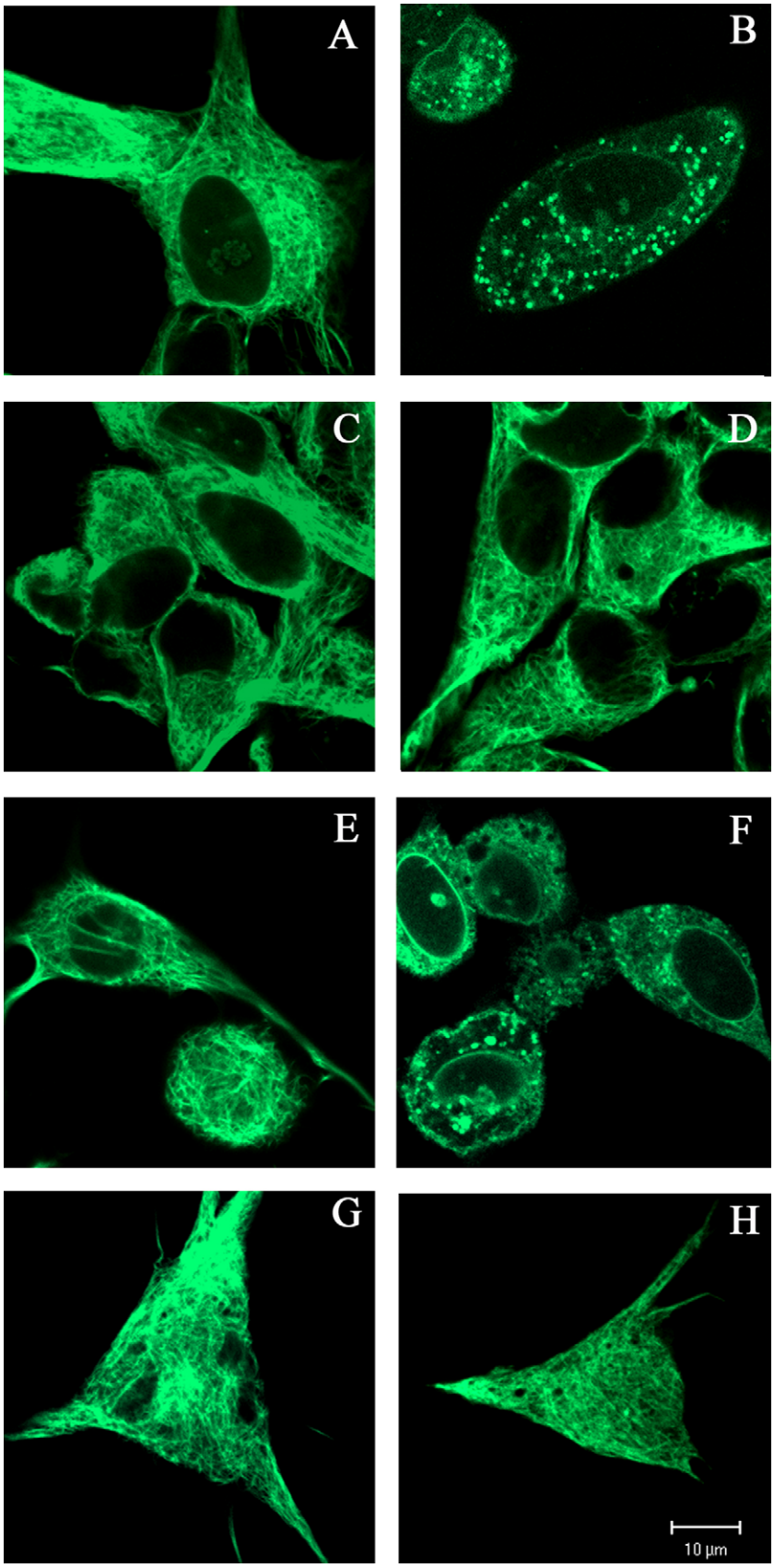

Fig. 4 – Microtubule structures of HEK rTRPV1/C2 cells in response to capsaicin treatment. Microtubule structures of HEK rTRPV1/C2 cells were studied by staining with TubulinTracker 10 min after the cells were treated with (A) DPBS buffer, (B) 200 nM capsaicin, (C) 10 μM A-425619, (D) 10 μM A-425619 alone for 5 min followed by 10 μM A-425619 + 200 nM capsaicin

disassembly, while it has no effect on microtubule structure by itself (Fig. 4C and D). When the extracellular calcium was chelated with 5 mM EGTA, microtubule fiber-like structure was not disrupted (Fig. 4E). Treatment with 200 nM of capsaicin and 5 mM EGTA together again caused microtubule depolymerization (Fig. 4F), which could be blocked by pretreatment of cells with 10 μM A-425619 (Fig. 4G–J) or 10 μM ruthenium red (data not shown).

3.5. *Cytosolic calcium redistribution in response to capsaicin treatment*

The above experiments clearly showed that capsaicin treatment induced protein synthesis inhibition and microtubule depolymerization in TRPV1-expressing cells. To correlate these events with alterations of cytosolic calcium levels, we studied the calcium changes in individual cells by confocal microscopy using live cell time series recordings. HEK rTRPV1/C2 cells were loaded with fluo-4 AM for 1 h before TRPV1 agonist or antagonist was applied. In calcium-containing medium, capsaicin treatment triggered calcium influx within 20 s. Over 95% of the cells responded to capsaicin stimulation (Fig. 5A). The strong green fluorescence sustained without significant decay for 20 min in most of the cells, only 5 out of 78 cells in the observation field showed abrupt reduction of fluorescent intensity between 10 and 20 min after capsaicin application, which is an indication of plasma membrane eruption. During the period of recording, the sizes of the cells, being measured based on the area at the scanning section, increased 25.2 ± 4.5% ($n = 7$) 500 s after capsaicin treatment, while no cell enlargement was observed (0.27 ± 1%, $n = 7$) when 10 μM of A-425619 was applied before capsaicin treatment (Table 1). 29.4% of the cells (20 out of 68 cells) exhibited significant shrinkage of cell processes after exposure to capsaicin, and this effect was blocked by pre-incubating cells with 10 μM A-425619 as well (Table 1).

When cells were incubated with 5 mM EGTA, 200 nM capsaicin treatment stimulated a couple of fluorescent sparks in each cell, but the overall signal intensities were very low, ranging from 2 to 20% of the signals observed in calcium-containing buffer (Fig. 5B). The onset of fluorescence started more than 50 s after capsaicin application, which is longer than that in calcium-containing buffer. Most of the fluorescent signals lasted less than 30 s (Fig. 5B). Five minutes after capsaicin application, fluorescence intensities of the cells were below the starting point. The reduction of fluorescent baseline suggested that, in the presence of 5 mM EGTA, 200 nM capsaicin-induced calcium flux was initiated from a limited calcium source (likely the intracellular calcium store) but not from an unlimited and uniform extracellular buffer system. Meanwhile, no significant changes were observed on the sizes of the cells over the period of capsaicin treatment, but the cell movement and the shrinkage of the cell processes were similar as those observed in calcium-containing buffer (Table 1).

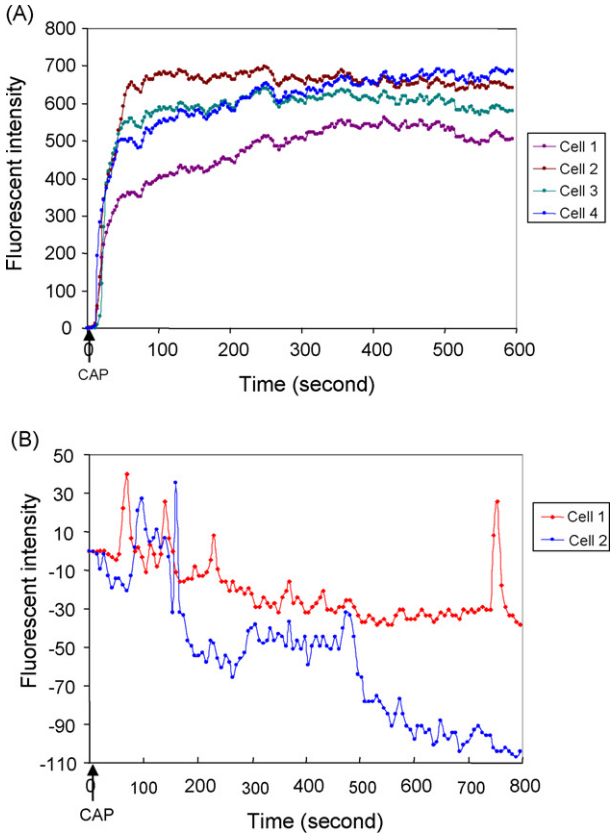

Fig. 5 – Capsaicin stimulates calcium flux from TRPV1 that are both on the plasma membrane and intracellular compartment. HEK rTRPV1/C2 cells that have been growing on chamber coverglasses for 2 days were loaded with flou-4 AM in DPBS buffer for 1 h before treatment. After removing the calcium dye, cells were replaced with DPBS buffer (A) or DPBS buffer with 5 mM EGTA (B) and were recorded under the Zeiss LSM5 PASCAL confocal microscope. Fluorescent images were captured every 3 s in (A) and 6 s in (B). Addition of 200 nM capsaicin was indicated with arrowheads on the *X*-axis. Fluorescence changes of the first 600 s for (A) and 800 s for (B) were presented. Baseline fluorescence at the starting point of recording was set at 0 for each cell. Traces of four representative cells in (A) and two representative cells in (B) were plotted against the function of time.

3.6. *eIF2α phosphorylation level did not change upon capsaicin treatment*

To study the mechanism leading to capsaicin-induced protein synthesis inhibition, we tested the eukaryotic initiation factor eIF2α phosphorylation level. As an important factor in peptide-chain initiation, eIF2α is regulated through phosphorylation in response to different stress conditions such as nutrition deprivation, viral double-stranded RNA, elevated

for another 10 min. Figures (E–H) are same treatments as those in (A–D), respectively, except that 5 mM of EGTA was included in all incubation. Representative fluorescent images taken with LSM5 PASCAL confocal microscope under 100× oil objective were shown. Bar = 10 μm.

Table 1 – Morphological changes of TRPV1 expressing cells upon capsaicin treatment

	Increment of cell size (%) ($n = 7$)	Shrinkage of cell processes	Microtubule structure
200 nM capsaicin	25.2 ± 4.4	29.4% (20 out of 68 cells)	Depolymerized
200 nM capsaicin + 10 μM A-425619	0.27 ± 1.1	1.7% (1 out of 60 cells)	Intact
200 nM capsaicin + 5 mM EGTA	2.6 ± 0.7	23.7% (18 out of 76 cells)	Depolymerized
200 nM capsaicin + 5 mM EGTA + 10 μM A-425619	−0.64 ± 0.76	6.3% (3 out of 48 cells)	Intact

Microtubule structure was determined using TubulinTracker. Size of the cell body was measured based on the area of each cell in the confocal microscopy scanning section, the percentages represented mean ± S.E.M. of area increment of seven cells after capsaicin treatment. Shrinkage of cell processes was measured as percentage of cells showed significant reduction on length of processes after capsaicin treatment in the observation filed. The number of cells with obvious process shrinkage and the number of total cells in the whole observation field are presented in parenthesis.

cellular calcium concentration and misfolded proteins to halt protein synthesis [35,36]. By using monoclonal antibodies that recognized total eIF2α and the phosphorylated form of eIF2α in Western blot analysis, we found that 200 nM of capsaicin treatment did not significantly induce eIF2α phosphorylation either in the presence or absence of extracellular calcium (Fig. 6). We therefore conclude that eIF2α phosphorylation is not the major mechanism for capsaicin-induced protein synthesis inhibition.

4. Discussion

TRPV1 is distributed both on the plasma membrane ($TRPV1_{PM}$) and intracellular membrane compartment, such as the ER ($TRPV1_{ER}$). Although the function and regulation of TRPV1 on the cell surface, whose activation directly correlates with membrane depolarization and neuron excitation has been studied extensively, the consequences of intracellular TRPV1 activation were not known. In this study, we investigated the contribution of the intracellular pool of TRPV1 to capsaicin-induced cytotoxicity. The studies in this report focused on two cellular processes, protein synthesis and microtubule integrity, both of which are highly sensitive

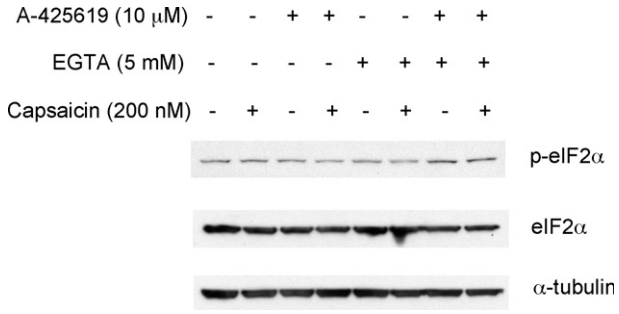

Fig. 6 – eIF2α phosphorylation state was not changed upon capsaicin treatment. Fifty micrograms of total cell lysates from HEK rTRPV1/C2 cells that were treated with 200 nM capsaicin, 5 mM EGTA, 10 μM A-425619 either alone or in different combinations for 60 min were fractionated on 4–12% Bis–Tris Nupage gel. The levels of phosphorylated and total eIF2α were detected by Western blot analysis using eIF2α phosphospecific antibody PHF0024 (1:200) and pan eIF2α antibody AHO0802 (1:1000). The level of α-tubulin showed equal loading of total protein in different lanes.

to calcium concentration. By comparing the protein synthesis rates and microtubule structures at the physiological calcium level, and at low-or-no extracellular calcium conditions, we demonstrated that calcium release from intracellular calcium stores through $TRPV1_{ER}$ activation was indeed sufficient to cause protein synthesis inhibition and microtubule depolymerization.

Capsaicin-induced cytotoxicity has been applied in clinical therapeutics long before its mechanism was known. Upon cloning of the capsaicin receptor TRPV1 in 1997 [1], understanding of the functional mechanisms of the receptor greatly improved. Previous studies have shown that the TRPV1 agonists capsaicin and Resiniferatoxin have strong cytotoxicities and cause protein synthesis inhibition, DNA fragmentation, membrane disruption and eventually cell death when applied to both TRPV1-expressing cells and even some cell types without TRPV1 expression. Unlike the TRPV1-independent cytotoxicity of capsaicin that usually requires higher concentration of capsaicin (25–100 μM) and longer exposure time (a few days) [22,23], capsaicin-induced protein synthesis inhibition and microtubule depolymerization in TRPV1-expressing cells are very potent and rapid. Moreover, these were reversed by treatment with the TRPV1 antagonist A-425619. Through application of TRPV1 antagonist and EGTA, we concluded that intracellular calcium mobilization is responsible for both of these cellular events.

Intracellular calcium homeostasis is important for normal cellular functions, such as metabolism, energy regeneration, structure integrity and trafficking processes [37–39]. In the resting state, cytosolic calcium is maintained at low concentration ($\sim 10^{-7}$ M) by the function of Ca-dependent ATPase, which pumps calcium from the cytosol to the extracellular medium or into intracellular calcium stores (ICS), such as the ER. During cell activation, calcium flows into the cytosol through calcium channels that are either located on the plasma membrane and/or endomembrane surrounding the ICS. These events are followed by rapid return back to resting level [40]. It has been well-documented in the paper by Karai et al. [27] that at least four sources contribute to vanilloid-stimulated $[Ca^{2+}]_i$ elevation: calcium influx from $TRPV1_{PM}$, calcium efflux from $TRPV1_{ER}$, calcium-induced calcium release (CICR) and store-operated calcium entry. We studied the calcium redistribution upon capsaicin treatment using live cell confocal microscopy. Instead of applying periodic stimulation, cells were incubated in agonist or antagonist containing buffer throughout the recording period. In normal calcium

buffer, drastic $[Ca^{2+}]_i$ elevation is observed upon capsaicin treatment (Fig. 5A). This correlated with 86% protein synthesis inhibition. Unlike the treatment with Resiniferatoxin that caused cell membrane burst and cell lysis within 2 min of exposure [37], no significant cell lysis was observed immediately after 200 nM capsaicin treatment, because strong intracellular calcium fluorescence was sustained over a period of 20 min. Thus, 73% of protein synthesis inhibition observed 20 min after capsaicin treatment was not the result of rapid cell lysis (Fig. 2A). In the presence of 5 mM EGTA, free calcium in the buffer system was reduced from 0.9 mM to 8 nM in the calcium imaging recordings and from 1.8 mM to 22 nM in the protein synthesis assay (calculated using EGTA calculator [33]). Under these conditions, calcium influx from extracellular sources and the subsequent CICR are not likely to occur in response to capsaicin stimulation. All of the calcium mobilization resulted from calcium efflux out of ER. The small and reoccurring peaks in response to capsaicin indicated repeated depletion and replenishing of calcium in the ER through $TRPV1_{ER}$ and other calcium channels located on ER. The reduced baselines upon treatment also confirmed that there is a finite source of calcium for each cell. This condition of calcium fluctuation correlated with 93% protein synthesis inhibition. When we included 10 μM ruthenium red together with 5 mM EGTA to ensure zero calcium influx from extracellular source [27], protein synthesis was not affected with 200 nM capsaicin treatment. The same result was obtained with A-425619 pre-treatment, which efficiently passes through plasma membrane and inhibits both $TRPV1_{PM}$ and $TRPV1_{EM}$. All these data suggest that elevation of cytosolic calcium from both extracellular sources and intracellular sources can inhibit protein synthesis. What is more, depletion of intracellular calcium store, such as ER, through activation of $TRPV1_{ER}$ is sufficient for protein synthesis inhibition.

Only high concentration (>20 μM) but not low concentration (<1 μM) of capsaicin was able to activate $TRPV1_{ER}$ in the presence of 10 μM ruthenium red according to what was reported in Karai's paper [27]. Mechanisms such as reduced agonist concentration in cytosolic compartments due to membrane binding or decreased accessibility of agonist to $TRPV1_{ER}$ were proposed to explain this phenomenon. In addition, we speculate that the increased threshold of capsaicin on $TRPV1_{ER}$ activation could be due to inhibition of $TRPV1_{ER}$ by ruthenium red that leaked into the cells. Ruthenium red is a negatively-charged molecule that is not cell permeable in many cell types in micro-imaging experiments. However, it is permeable through the neuron plasma membrane [41]. The penetration through non-neuronal cells such as HEK293 cells could be much weaker, but may not be absolutely exclusive. Since ruthenium red is a potent channel blocker, residual amounts in the cell may be sufficient to decrease channel conductance. The reduced potency for capsaicin to stimulate $TRPV1_{ER}$ in the presence of ruthenium red is consistent with this hypothesis.

Calcium can inhibit protein synthesis through different mechanisms depending on which pool of calcium is altered. Isolated elevation of cytoplasmic calcium blocks protein synthesis at the peptide elongation step [42], while calcium depletion from the ER inhibits protein synthesis at the translation initiation step. Thapsigargin (TG), an irreversible inhibitor of ER Ca-dependent ATPase that pumps calcium from cytosol into ER, induces polyribosome disaggregation and translation initiation blockade [43]. Moreover, the eIF2α phosphorylation state increases 2–3-fold, which is also believed to repress translation initiation [35]. The consequence of $TRPV1_{ER}$ activation is similar to Ca-dependent ATPase inhibition by Thapsigargin in that they both result in calcium depletion from ER and calcium overload in cytosol [27]. To figure out the mechanism by which capsaicin inhibits protein synthesis, we checked the phosphorylation status of eIF2α. However, under conditions that correlated with either protein synthesis or protein synthesis inhibition, no significant changes of eIF2α phosphorylation was observed. Due to the presence of both $TRPV1_{PM}$ and $TRPV1_{ER}$, intracellular calcium status differs depends on extracellular calcium conditions. So we speculate that, under normal extracellular calcium level, capsaicin primarily causes drastic elevation of cytosolic calcium through $TRPV1_{PM}$ and $TRPV1_{ER}$, but ER calcium is not depleted because of calcium reentry through channels like Ca-dependent ATPase on ER, therefore, protein synthesis is likely blocked at peptide elongation step. Under zero $[Ca^{2+}]_o$ condition, capsaicin causes calcium depletion from ER and the transient calcium overload in cytosol, protein synthesis is likely blocked at the translation initiation step, but not through phosphorylation of eIF2α.

Microtubules are one of the major components of the cytoskeleton. Microtubule structure is not only correlated with cell morphology, but also constitutes a network for vesicle trafficking in the cells. In neurons, whose cell bodies are very far away from the processes terminals, microtubule-mediated protein trafficking is crucial since the neuron terminals are the sites for cell signaling and cell–cell interaction. Microtubule disassembly is cytotoxic because it causes vesicle accumulation and impairs neurotransmitters release [44]. Capsaicin-induced microtubule depolymerization was initially reported in Goswami et al. [45]. In our study, instead of using tubulin antibody, we used TubulinTracker that only binds with polymerized microtubules to observe microtubule structures. Dramatic differences were observed before and after capsaicin treatment by confocal microscopy. Microtubules disassembled upon elevation of cytosolic calcium originating from either extracellular sources or from intracellular calcium stores. The TRPV1 specific antagonist A-425619 and the non-selective channel antagonist ruthenium red, that completely block intracellular calcium elevation, also reversed capsaicin-induced microtubule disassembly. Comparing the changes of cell size and the shrinkage of cell processes with the integrity of microtubules upon capsaicin treatment, we found the shrinkage of cell processes correlated more tightly with depolymerization of microtubule structure, while the swelling of cells was not as relevant and could be due to osmotic effect. Thus, it is possible that shrinkage of cell processes could rapidly terminate signal transduction mediated via synaptic contact between neurons through capsaicin-induced microtubule disassembly. It also suggests a self-defense mechanism in neurons to quickly terminate the excitatory signals through regulation of neuron morphology.

Although protein synthesis and microtubule disassembly seem quite disconnected, they are actually closely related cellular processes. It has been reported that microtubules and

the ER are interdependent organelles. Attachment of the ER to the microtubule cytoskeleton is a prerequisite for ER maintenance [46]. In addition, microtubules also function as a docking framework for translational machinery. Messenger RNA, ribosomal and polyribosome proteins were reported to associate with microtubules to ensure efficient protein translation [47–49]. Collapse of microtubules could directly affect protein synthesis simply by disassembling the components of translational machinery. This provides an explanation for the concurrent events of protein synthesis inhibition and microtubule depolymerization during capsaicin stimulation. However, microtubule integrity is not the only factor for normal protein synthesis, because protein synthesis inhibition was not reversed when we stabilize microtubules with Taxol before capsaicin treatment (data not shown), suggesting that other component(s) were also required.

In summary, this study investigated the mechanisms of TRPV1-mediated cytotoxicities and revealed the role and contribution of intracellular TRPV1 in capsaicin-induced protein synthesis inhibition and microtubule depolymerization. Our study provides molecular basis for physiological consequences of TRPV1 activation, thus enabling a better understanding of TRPV1 as a therapeutic target for pain sensation.

REFERENCES

[1] Caterina MJ, Schumacher MA, Tominaga M, Rosen TA, Levine JD, Julius D. The capsaicin receptor: a heat-activated ion channel in the pain pathway. Nature 1997;389:816–24.

[2] Tominaga M, Caterina MJ, Malmberg AB, Rosen TA, Gilbert H, Skinner K, et al. The cloned capsaicin receptor integrates multiple pain-producing stimuli. Neuron 1998;21:531–43.

[3] Ryu S, Liu B, Qin F. Low pH potentiates both capsaicin binding and channel gating of VR1 receptors. J Gen Physiol 2003;122:45–61.

[4] Birder LA, Kanai AJ, de Groat WC, Kiss S, Nealen ML, Burke NE, et al. Vanilloid receptor expression suggests a sensory role for urinary bladder epithelial cells. Proc Natl Acad Sci USA 2001;98:13396–401.

[5] Kido MA, Muroya H, Yamaza T, Terada Y, Tanaka T. Vanilloid receptor expression in the rat tongue and palate. J Dent Res 2003;82:393–7.

[6] Roberts JC, Davis JB, Benham CD. [3H]Resiniferatoxin autoradiography in the CNS of wild-type and TRPV1 null mice defines TRPV1 (VR-1) protein distribution. Brain Res 2004;995:176–83.

[7] Caterina MJ, Leffler A, Malmberg AB, Martin WJ, Trafton J, Petersen-Zeitz KR, et al. Impaired nociception and pain sensation in mice lacking the capsaicin receptor. Science 2000;288:306–13.

[8] Davis JB, Gray J, Gunthorpe MJ, Hatcher JP, Davey PT, Overend P, et al. Vanilloid receptor-1 is essential for inflammatory thermal hyperalgesia. Nature 2000;405:183–7.

[9] Honore P, Wismer CT, Mikusa J, Zhu CZ, Zhong C, Gauvin DM, et al. A-425619 [1-isoquinolin-5-yl-3-(4-trifluoromethyl-benzyl)-urea], a novel transient receptor potential type V1 receptor antagonist, relieves pathophysiological pain associated with inflammation and tissue injury in rats. J Pharmacol Exp Ther 2005;314:410–21.

[10] Gomtsyan A, Bayburt EK, Schmidt RG, Zheng GZ, Perner RJ, Didomenico S, et al. Novel transient receptor potential vanilloid 1 receptor antagonists for the treatment of pain: structure–activity relationships for ureas with quinoline, isoquinoline, quinazoline, phthalazine, quinoxaline, and cinnoline moieties. J Med Chem 2005;48:744–52.

[11] Culshaw AJ, Bevan S, Christiansen M, Copp P, Davis A, Davis C, et al. Identification and biological characterization of 6-aryl-7-isopropylquinazolinones as novel TRPV1 antagonists that are effective in models of chronic pain. J Med Chem 2006;26:471–4.

[12] Ognyanov VI, Balan C, Bannon AW, Bo Y, Dominguez C, Fotsch C, et al. Design of potent, orally available antagonists of the transient receptor potential vanilloid 1, structure–activity relationships of 2-piperazin-1-yl-1H-benzimidazoles. J Med Chem 2006;49:3719–42.

[13] Shin J, Cho H, Hwang SW, Jung J, Shin CY, Lee SY, et al. Bradykinin-12-lipoxygenase-VR1 signaling pathway for inflammatory hyperalgesia. Proc Natl Acad Sci USA 2002;99:10150–5.

[14] Huang SM, Bisogno T, Trevisani M, Al-Hayani A, De Petrocellis L, Fezza F, et al. An endogenous capsaicin-like substance with high potency at recombinant and native vanilloid VR1 receptors. Proc Natl Acad Sci USA 2002;99:8400–5.

[15] Chu CJ, Huang SM, De Petrocellis L, Bisogno T, Ewing SA, Miller JD, et al. N-Oleoyldopamine, a novel endogenous capsaicin-like lipid that produces hyperalgesia. J Biol Chem 2003;278:13633–9.

[16] Jancso G, Kiraly E, Jancso-Gabor A. Pharmacologically induced selective degeneration of chemosensitive primary sensory neurones. Nature 1977;270:741–3.

[17] Yaksh TL, Farb DH, Leeman SE, Jessell TM. Intrathecal capsaicin depletes substance P in the rat spinal cord and produces prolonged thermal analgesia. Science 1979;206:481–3.

[18] Winter J, Dray A, Wood JN, Yeats JC, Bevan S. Cellular mechanism of action of resiniferatoxin: a potent sensory neuron excitotoxin. Brain Res 1990;520:131–40.

[19] Karai L, Brown DC, Mannes AJ, Connelly ST, Brown J, Gandal M, et al. Deletion of vanilloid receptor 1-expressing primary afferent neurons for pain control. J Clin Invest 2004;113:1344–52.

[20] Szallasi A, Blumberg PM. Vanilloid (capsaicin) receptors and mechanisms. Pharmacol Rev 1999;51:159–212.

[21] Cruz F. Mechanisms involved in new therapies for overactive bladder. Urology 2004;63:65–73.

[22] Creppy EE, Richeux F, Carratu MR, Cuomo V, Cochereau C, Ennamany R, et al. Cytotoxicity of capsaicin in monkey kidney cells: lack of antagonistic effects of capsazepine and ruthenium red. Arch Toxicol 2000;74:40–7.

[23] Richeux F, Cascante M, Ennamany R, Saboureau D, Creppy EE. Cytotoxicity and genotoxicity of capsaicin in human neuroblastoma cells SHSY-5Y. Arch Toxicol 1999;73:403–9.

[24] Reilly CA, Taylor JL, Lanza DL, Carr BA, Crouch DJ, Yost GS. Capsaicinoids cause inflammation and epithelial cell death through activation of vanilloid receptors. Toxicol Sci 2003;73:170–81.

[25] Reilly CA, Johansen ME, Lanza DL, Lee J, Lim JO, Yost GS. Calcium-dependent and independent mechanisms of capsaicin receptor (TRPV1)-mediated cytokine production and cell death in human bronchial epithelial cells. J Biochem Mol Toxicol 2005;19:266–75.

[26] Liu M, Liu MC, Magoulas C, Priestley JV, Willmott NJ. Versatile regulation of cytosolic Ca2+ by vanilloid receptor I in rat dorsal root ganglion neurons. J Biol Chem 2003;278:5462–72.

[27] Karai LJ, Russell JT, Iadarola MJ, Olah Z. Vanilloid receptor 1 regulates multiple calcium compartments and contributes

to Ca2+-induced Ca2+ release in sensory neurons. J Biol Chem 2004;279:16377–8.
[28] Vos HM, Neelands TR, McDonald HA, Choi W, Kroeger PE, Puttfarcken PS, et al. TRPV1b overexpression negatively regulates TRPV1 responsiveness to capsaicin, heat and low pH in HEK293 cells. J Neurochem 2006;99:1088–102.
[29] Witte DG, Cassar SC, Masters JN, Esbenshade T, Hancock AA. Use of a fluorescent imaging plate reader-based calcium assay to assess pharmacological differences between the human and rat vanilloid receptor. J Biomol Screen 2002;7:466–75.
[30] McGaraughty S, Chu KL, Bitner RS, Martino B, El Kouhen R, Han P, et al. Capsaicin infused into the PAG affects rat tail flick responses to noxious heat and alters neuronal firing in the RVM. J Neurophysiol 2003;90:2702–10.
[31] Brostrom MA, Brostrom C. Calcium dynamics and endoplasmic reticular function in the regulation of protein synthesis: implications for cell growth and adaptability. Cell Calcium 2003;34:345–63.
[32] El Kouhen R, Surowy CS, Bianchi BR, Neelands TR, McDonald HA, Niforatos W, et al. A-425619 [1-isoquinolin-5-yl-3-(4-trifluoromethyl-benzyl)-urea], a novel and selective transient receptor potential type V1 receptor antagonist, blocks channel activation by vanilloids, heat, and acid. J Pharmacol Exp Ther 2005;314:400–9.
[33] Portzehl H, Caldwell PC, Rueegg JC. The dependence of contraction and relaxation of muscle fibers from the crab maia squinado on the internal concentration of free calcium ions. Biochim Biophys Acta 1964;79:581–91.
[34] Diaz JF, Barasoain I, Andreu JM. Fast kinetics of Taxol binding to microtubules. Effects of solution variables and microtubule-associated proteins. J Biol Chem 2003;278:8407–19.
[35] Prostko CR, Brostrom MA, Malara EM, Brostrom CO. Phosphorylation of eukaryotic initiation factor (eIF) 2 alpha and inhibition of eIF-2B in GH3 pituitary cells by perturbants of early protein processing that induce GRP78. J Biol Chem 1992;267:16751–4.
[36] Taylor SS, Haste NM, Ghosh G. PKR and eIF2alpha: integration of kinase dimerization, activation, and substrate docking. Cell 2005;122:823–5.
[37] Olah Z, Szabo T, Karai L, Hough C, Fields RD, Caudle RM, et al. Ligand-induced dynamic membrane changes and cell deletion conferred by vanilloid receptor 1. J Biol Chem 2001;276:11021–30.
[38] Hail Jr N. Mechanisms of vanilloid-induced apoptosis. Apoptosis 2003;8:251–62.
[39] Jambrina E, Alonso R, Alcalde M, del Carmen Rodriguez M, Serrano A, Martinez-A C, et al. Calcium influx through receptor-operated channel induces mitochondria-triggered paraptotic cell death. J Biol Chem 2003;278:14134–45.
[40] Alvarez J, Montero M, Garcia-Sancho J. Subcellular Ca(2+) dynamics. News Physiol Sci 1999;14:161–8.
[41] Tapia R, Velasco I. Ruthenium red as a tool to study calcium channels, neuronal death and the function of neural pathways. Neurochem Int 1997;30:137–47.
[42] Wong WL, Brostrom MA, Brostrom CO. Effects of Ca2+ and ionophore A23187 on protein synthesis in intact rabbit reticulocytes. Int J Biochem 1991;23:605–8.
[43] Doutheil J, Gissel C, Oschlies U, Hossmann KA, Paschen W. Relation of neuronal endoplasmic reticulum calcium homeostasis to ribosomal aggregation and protein synthesis: implications for stress-induced suppression of protein synthesis. Brain Res 1997;775:43–51.
[44] Goldstein LS. Do disorders of movement cause movement disorders and dementia? Neuron 2003;40:415–25.
[45] Goswami C, Dreger M, Otto H, Schwappach B, Hucho F. Rapid disassembly of dynamic microtubules upon activation of the capsaicin receptor TRPV1. J Neurochem 2006;96:254–66.
[46] Vedrenne C, Hauri HP. Morphogenesis of the endoplasmic reticulum: beyond active membrane expansion. Traffic 2006;7:639–46.
[47] Hamill D, Davis J, Drawbridge J, Suprenant KA. Polyribosome targeting to microtubules: enrichment of specific mRNAs in a reconstituted microtubule preparation from sea urchin embryos. J Cell Biol 1994;127:973–84.
[48] O'Brien Jr JM, Wewers MD, Moore SA, Allen JN. Taxol and colchicine increase LPS-induced pro-IL-1 beta production, but do not increase IL-1 beta secretion. A role for microtubules in the regulation of IL-1 beta production. J Immunol 1995;154:4113–22.
[49] Zhou B, Rabinovitch M. Microtubule involvement in translational regulation of fibronectin expression by light chain 3 of microtubule-associated protein 1 in vascular smooth muscle cells. Circ Res 1998;83:481–9.